Journal of Autism and Developmental Disorders, Vol. 31, No. 6, December 2001 (© 2001)

Magnetic Resonance Imaging of the Post-Mortem Autistic Brain

Cynthia Mills Schumann,[1] Michael H. Buonocore,[2] and David G. Amaral[1,3]

Magnetic resonance imaging (MRI) is a valuable, noninvasive tool for understanding structural abnormalities in the brain. The M.I.N.D. Institute at UC Davis has developed a protocol utilizing MRI to investigate anatomical differences in the post-mortem brain by applying a proton density weighted imaging sequence for optimal differences in image intensity (contrast) between gray and white matter. Images of the brain obtained prior to distribution of tissue and further neuropathological examination provide a record of how the brain appeared prior to tissue processing. The virtual representation of the whole brain can also be subjected to additional analyses, such as measuring the volume of brain regions or area of the cortical surface. We describe our procedures for carrying out post-mortem MRI of the human brain.

KEY WORDS: Autism; MRI; neuroimaging.

INTRODUCTION

Many studies in the autism literature have utilized magnetic resonance imaging (MRI) as a method for studying volumetric differences in the brains of autistic subjects versus those of typically developing children. Reports from such studies include an increase in total brain volume (Piven *et al.,* 1996), and cerebellar and parietal lobe abnormalities (Saitoh & Courchesne, 1998). MRI has also proved to be a sensitive tool for assessing white matter changes and cerebral atrophy both in living subjects (Seab *et al.,* 1988; Jack *et al.*, 1992) as well as in the post-mortem brain (Bobinski *et al.,* 2000) in disorders such as Alzheimer's disease. Many dementia patients are enrolled in formal research programs prior to death and therefore pre-mortem MRIs are often available for brains acquired for tissue analysis. This is not the case, however, in autism. Brain tissue is acquired only through accidental death and tissue is distributed through organizations such as the Autism Tissue Program (ATP). Because autism is a heterogeneous disorder with no known cause, researchers currently are interested in studying several areas of the brain. Therefore, the tissue from an individual brain is often distributed to many researchers for analysis. MRI provides an ideal method for retaining a virtual three-dimensional representation of the intact brain. This representation may allow analyses that would not be possible after the brain has been blocked for histological investigation. For example, in one post-mortem sample of autistic brain tissue, Bailey and colleagues (1998) noted large, hyperconvoluted temporal lobes and upwardly rotated hippocampi. These types of changes may be missed in brains that are simply blocked and distributed for histological analysis. Sulcal abnormalities could be formally and quantitatively assessed using MRI images of post-mortem brains.

To our knowledge, there have not been any reports utilizing MRI on post-mortem human brains in autism

[1] The M.I.N.D. Institute, Department of Psychiatry, and Center for Neuroscience, University of California, Davis.
[2] Department of Radiology, University of California, Davis, School of Medicine.
[3] Correspondence should be addressed to: David G. Amaral, Ph.D., Center for Neuroscience, University of California, Davis, 1544 Newton Ct., Davis, CA 95616; Tel.: (530) 757-8813; Fax: (530) 754-7016; e-mail: dgamaral@ucdavis.edu

0162-3257/01/1200-0561/0

research. However, MRI has been found to be beneficial in post-mortem studies of other neurological disorders, including multiple sclerosis (Nagara *et al.*, 1987), tuberous sclerosis (Nixon *et al.*, 1989), and the morphology of white matter changes in aging (Scarpelli *et al.*, 1994). These studies relied primarily on T1- and T2-weighted images. However, in formalin fixed brains, white and gray matter had similar image intensities and were difficult to distinguish. The inability to distinguish white and gray matter after fixation on the basis of T1 and T2 weighted images can be explained in terms of the underlying biophysical mechanism that determines the T1 and T2 of a tissue. T1 (longitudinal) and T2 (transverse) relaxation times of hydrogen protons rely on the mobility of water within the tissue. Fixatives such as formalin act by cross-linking proteins, which tends to reduce differences in water mobility among different tissue types in the brain. Tovi & Ericsson (1992) demonstrated that the most rapid decline of T1 occurred during the first 2 weeks of fixation and continued to decline in successive weeks, leading to reduced tissue contrast in T1-weighted images. However, differences in the relative density of protons within these tissue types increases with fixation, suggesting that proton-density weighted images will show greater tissue contrast compared to T1- or T2-weighted images. Blamire and colleagues (1999) demonstrated systematic changes in the brain during formalin fixation over a period of 5 weeks. Specifically, there was a significant decrease in the T2 times of gray and white matter, and a significant decrease in the ratio of T2 times of gray matter to white matter, within the first week of fixation that continued to decline, reaching a plateau by the fifth week. These results suggested that T2-weighted images would show less contrast between gray and white matter than routinely obtained in *in vivo* brain imaging. Conversely, Blamire and colleagues (1999) showed a significant increase in the ratio of proton densities of gray to white matter after the first week of fixation and continued to increase over successive weeks. These results suggested that proton density-weighted images would result in higher contrast between gray and white matter in formalin fixed brains.

METHODS

Due to the effects of fixation, typical clinical protocols that are optimal for imaging living human brains *in vivo* are not optimal for imaging post mortem brains. We confirmed this by attempting several standard T1 and T2 imaging sequences on the post mortem brain; all produced poor gray matter/white matter contrast. A proton density-weighted imaging sequence, as shown in Table I, with long repetition time (TR) and short echo time (TE) was developed for optimal contrast between gray and white matter in the post-mortem brain. Eight whole brains and six hemispheres were used for our analysis. The duration of formalin fixation prior to MRI ranged from 6 weeks to 15 months.

One complication of post-mortem brain imaging is that the brain must remain moist for the duration of the scan to preserve tissue properties. However, if the brain is submerged in liquid, the surface of the brain on the image cannot be easily distinguished from the liquid in which it is submerged. We have devised a successful method of keeping the brain moist while acquiring images. A Plexiglas (22 × 17 × 17 cm) container and various supporting structures were constructed (Fig. 1). At the time of imaging, warm water (approximately 120°F) was placed into the bottom of the container below the support structure. The brain was then supported so as to be in a standardized orientation and the lid was securely closed. This container provided a humid environment in which the brain could remain for the hour or more that was essential for carrying out the scan without any dehydration of the surface. All scans were performed on a 1.5 Tesla GE NV/I MRI System (GE Medical Systems, Waukesha, WI) at the UC Davis Imaging Center.

A fast spin echo (FSE) sequence was chosen because it provided reasonable scan times despite long TR, set to 6700 ms, which allowed for the elimination

Table I. Proton Density-Weighted Pulse Sequence Applied for Magnetic Resonance Imaging on Post-Mortem Brain Tissue

Sequence	Fast spin echo (FSE)
Slice Orientation	Coronal
Contrast Weighting	Proton Density
Repetition Time (TR)	6700 ms
Effective Echo Time (TE)	8.23 ms
Echo Train Length (ETL)	4
Number of Slices	114
Slice Thickness	1.6 mm
Interslice Gap	0.0 mm
FOV	16 cm × 16 cm
Matrix	256 (Phase Encode) × 512 (Freq. Encode)
In-plane Resolution	625 microns × 312.5 microns
Number of Excitations (NEX)	7
Bandwidth (BW)	62.5 kHz
Total Scan Time	50 minutes, 29 seconds
Options:	
Tailored RF pulses (TRF)	On
Zero-fill interpolation (ZIP)	To 512 × 512 image matrix

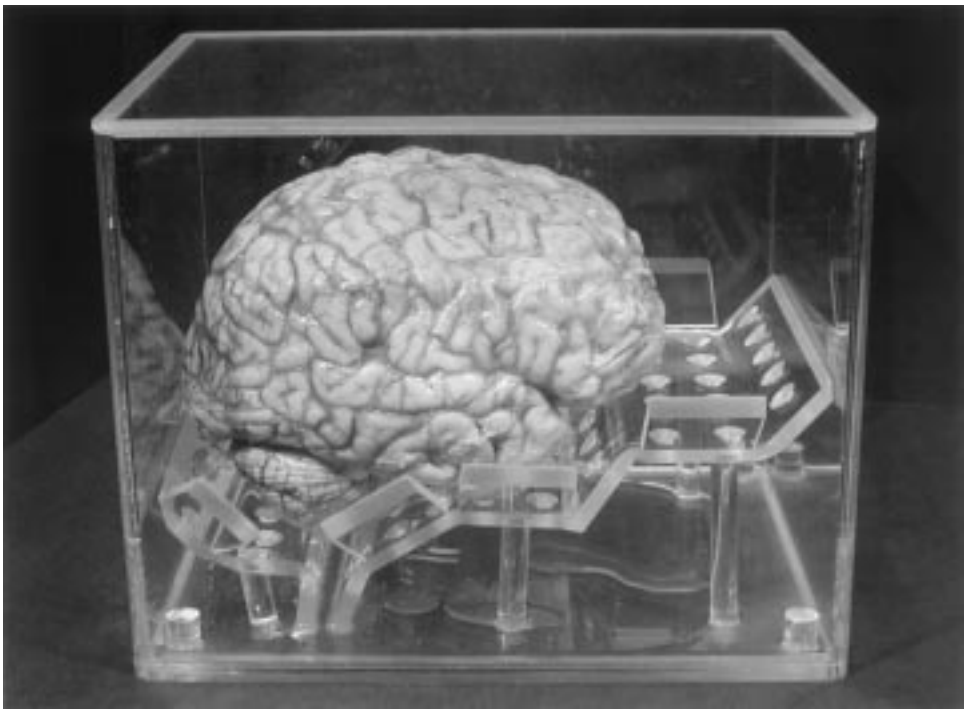

Fig. 1. Post-mortem brain in Plexiglas container (22 × 17 × 17 cm) constructed for MRI. The brain is supported by platforms to maintain alignment along the horizontal axis between anterior and posterior commissures (AC-PC).

of T1 weighting and the acquisition of a large number of slices, 114 in one acquisition. The echo train length (ETL) was set to 4, and effective TE set to the minimum (8.23 ms). The combination of ETL = 4 and 114 slices provided full use of the TR interval for generating data. Slice thickness was set at 1.6 mm and 0 mm interslice gap, which allowed full coverage of the brain with coronal slices. Normally a small gap is recommended, such as 0.1-mm gap with 1.5-mm thickness. However, 0 mm gap ensured that all tissue was represented in the image set, and a separate investigation of the overlap of adjacent slices showed that both specifications, 0.1 mm gap and 0 mm gap, had appreciable overlap of 20% to 30%. Therefore, image quality was comparable in the two cases. The tailored RF pulse option (TRF) was used to improve slice profiles and, in particular, to improve the sharpness of the edges of each slice. Although three-dimensional FSE was considered, it was deemed sub-optimal for this application because the ETL needed to be small to maximize signal and minimize T2 weighting. Field of view was set to 16 cm to include the entire cross-section of the brain without risk of wrap-around artifact. A high-resolution k-space data set was acquired, consisting of 256 points in the phase encode direction and 512 points in the frequency encode direction. In-plane voxel dimensions were 625.0 microns × 312.5 microns. Image post-processing included zero fill interpolation to 512 matrix in the phase encode direction, which improved the definition of curved edges, which is important for segmentation. The small voxel dimensions necessitated signal averaging to improve signal-to-noise ratio. The number of repeated excitations (NEX) was set to 7. Bandwidth was set to a relatively high value of 62.5 kHz which, relative to the usual 32 kHz, lowered the signal-to-noise ratio but was necessary for short TE. The total scan time is 50 minutes 29 seconds.

RESULTS

An MRI coronal section from a proton density weighted pulse sequence of a post-mortem brain (autistic male, age 14) is displayed in Fig. 2, demonstrating the contrast and resolution obtained after the brain was fixed for 3 months in 10% buffered formalin. The difference in proton densities with tissue fixation result in white matter appearing dark, gray matter appearing light, and fluid appearing brightest in the image.

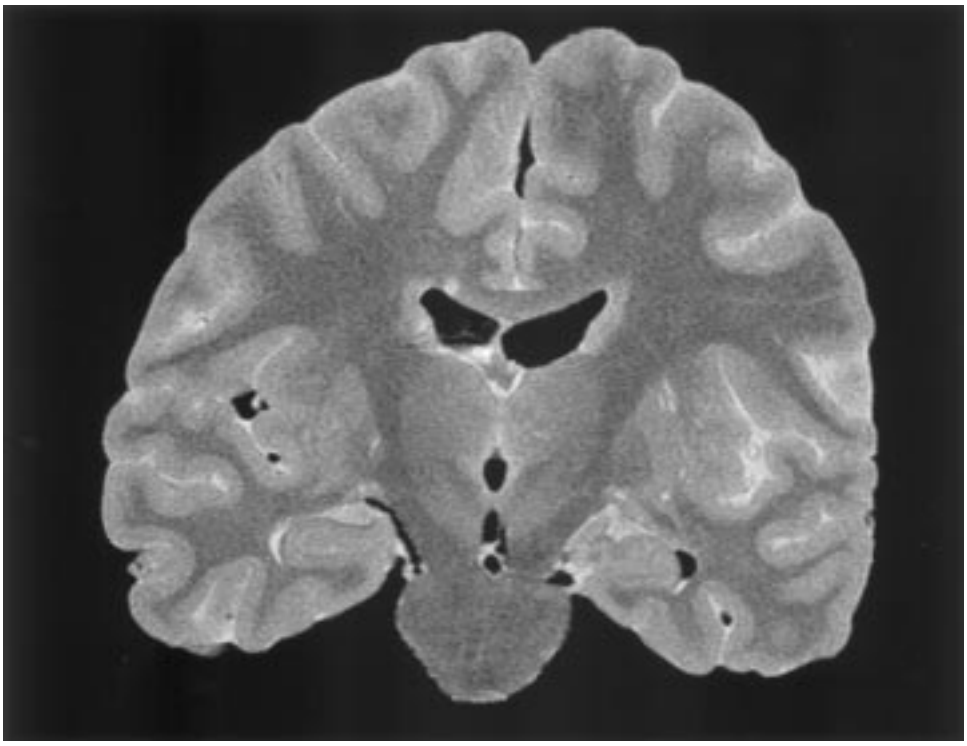

Fig. 2. Coronal slice from a proton density-weighted MRI scan of a post-mortem brain (autistic male, age 14) displaying contrast and resolution obtained after 3 months of fixation.

The brain is susceptible to distortion at many steps prior to histological examination, which may be revealed in the MRI scan. Large, deep cuts commonly occur during removal of the brain from the skull (Fig. 3A), but may go unnoticed in a frozen block of tissue. Fig. 3B illustrates where a section of tissue was removed from the cerebellum prior to imaging. Another common problem occurs when the brain is not properly fixed. Internal structures will be soft and lose structural integrity. This type of distortion may be detected in an MRI scan prior to blocking the tissue. The bright signal in Fig. 3C was consistent with an area of poorly fixed tissue when the brain was blocked. Although identification of these poorly fixed areas does not necessarily lead to any action to better preserve the brain (because degradation of the brain will be irreversible at this point), it may preclude unproductive effort to prepare these regions for histological analysis.

Post-mortem MRI may also provide a possible mechanism for volumetric analysis (Bobinski *et al.*, 2000) and three-dimensional surface maps of the brain. VirtualSurgery, a program currently being developed by Evan Fletcher at the Center for Neuroscience, UC Davis, is designed to reconstruct a set of MRI slices. By utilizing this program, we are able to preserve a three-dimensional record of each brain prior to sectioning. The program is then capable of subtracting areas of the brain in the reconstructed image to view internal structures for each individual brain, thereby providing a powerful tool for comparing histological findings with the gross brain. Fig. 4 is a three-dimensional reconstruction of an MRI scan from the brain in the Plexiglas container shown in Fig. 1. Although proton density–weighted images on fixed post-mortem brains result in dark white matter and light gray matter, the color scale has been inverted to present a more typical anatomical appearance. The transverse plane through panel (A) in Fig. 4 displays the location where the first cut was made on the three-dimensional image to create the picture shown in panel (B). After making the first cut, internal structures such as the amygdala can be observed in the image. A second cut was made further caudal through the hippocampus, shown in panel (C).

DISCUSSION

To report accurate anatomical abnormalities in the autistic brain, it is helpful to obtain high-quality MRI images prior to distribution of the tissue. Our study sug-

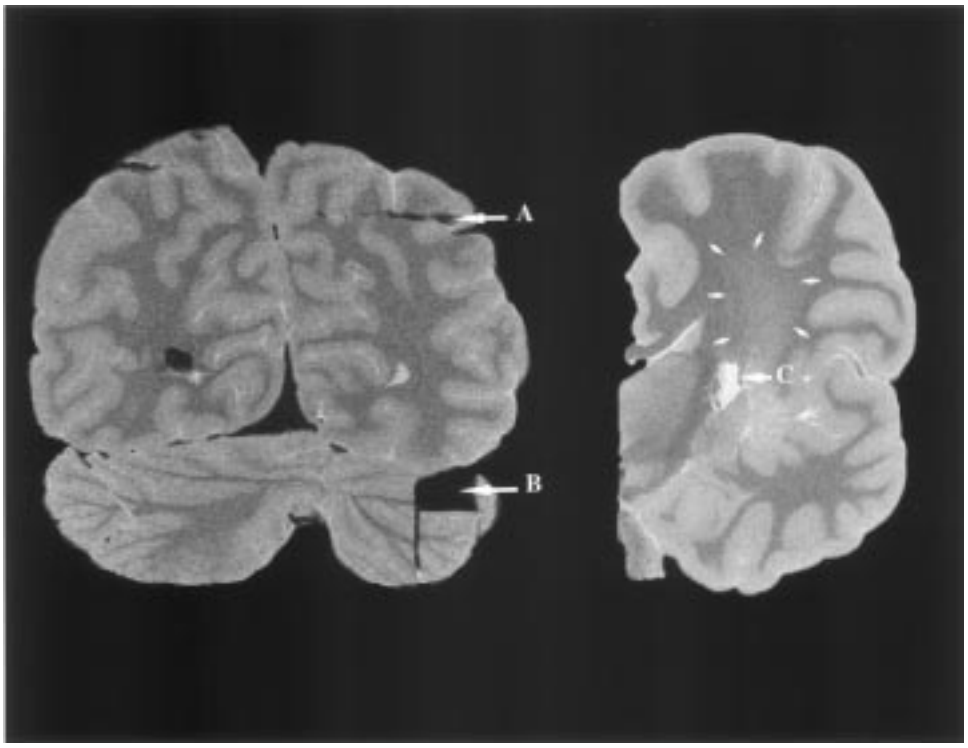

Fig. 3. Examples of distortion commonly observed in post-mortem brains. (right) MRI coronal slice of a whole brain (male, age 44) and (left) coronal slice of a hemisphere (autistic male, age 26). Deep cuts (A) often occur during removal of the brain from the skull. Tissue sections (B) may also be removed for neuropathological examination, as seen here in the cerebellum. Insufficient fixation of brain tissue (C) may also be observed in a proton density-weighted image by abnormally bright signal intensity in deep tissue.

gests that typical clinical MRI parameters, with T1 and T2 weighting, result in reduced contrast in fixed tissue. By utilizing a proton density weighted sequence for MRI, it is possible to generate high-resolution and high gray/white matter contrast images of the post-mortem brain.

Future studies of the post-mortem brain should consider an optimal balance between imaging time verses anatomical resolution. With a slice thickness of 1.6 mm and in-plane resolution of 0.625×0.3125 mm, the data set is relatively low resolution in the slice select direction and, therefore, is unable to provide reformatted images with the same in-plane spatial resolution as the original images. A data set with uniform resolution in all directions would be most desirable for analysis of any brain structure. Imaging a nonliving object provides the advantage of being able to lengthen the scan time to several hours or more to achieve higher resolution in the slice select direction. For example, increasing the number of slices by a factor of three, to 342, would allow full brain coverage with a slice thickness of 0.533 mm. Due to the decreased voxel size, the signal-to-noise (SNR) would decrease by a factor of sqrt(3), and the scan time would increase by a factor of three. This SNR loss could be recovered using a factor of three increase in NEX. Thus, under this scheme the scan time increases by a factor of nine, to 7 hours, 34 minutes, 21 seconds. A factor of two reductions in slice thickness, to 0.8 mm, would require a factor of four increase in scan time, to 3 hours, 21 minutes, 56 seconds. These are practical scan times for nonliving tissue provided that the water content and dimension of the tissue remains constant through the duration of the scan. Although it has not been evaluated, it is believed that the closed Plexiglas container provides this constant water content and dimension of the tissue.

Although the single three-dimensional acquisitions described are the most efficient for increasing resolution while maintaining SNR, they cannot be implemented with current commercial GE pulse sequences. Due to a software limitation, specifying greater than 124 slices in a three-dimensional acquisition is currently not possible on the GE MRI system. Therefore, to acquire the data set with 0.533 mm slice thickness

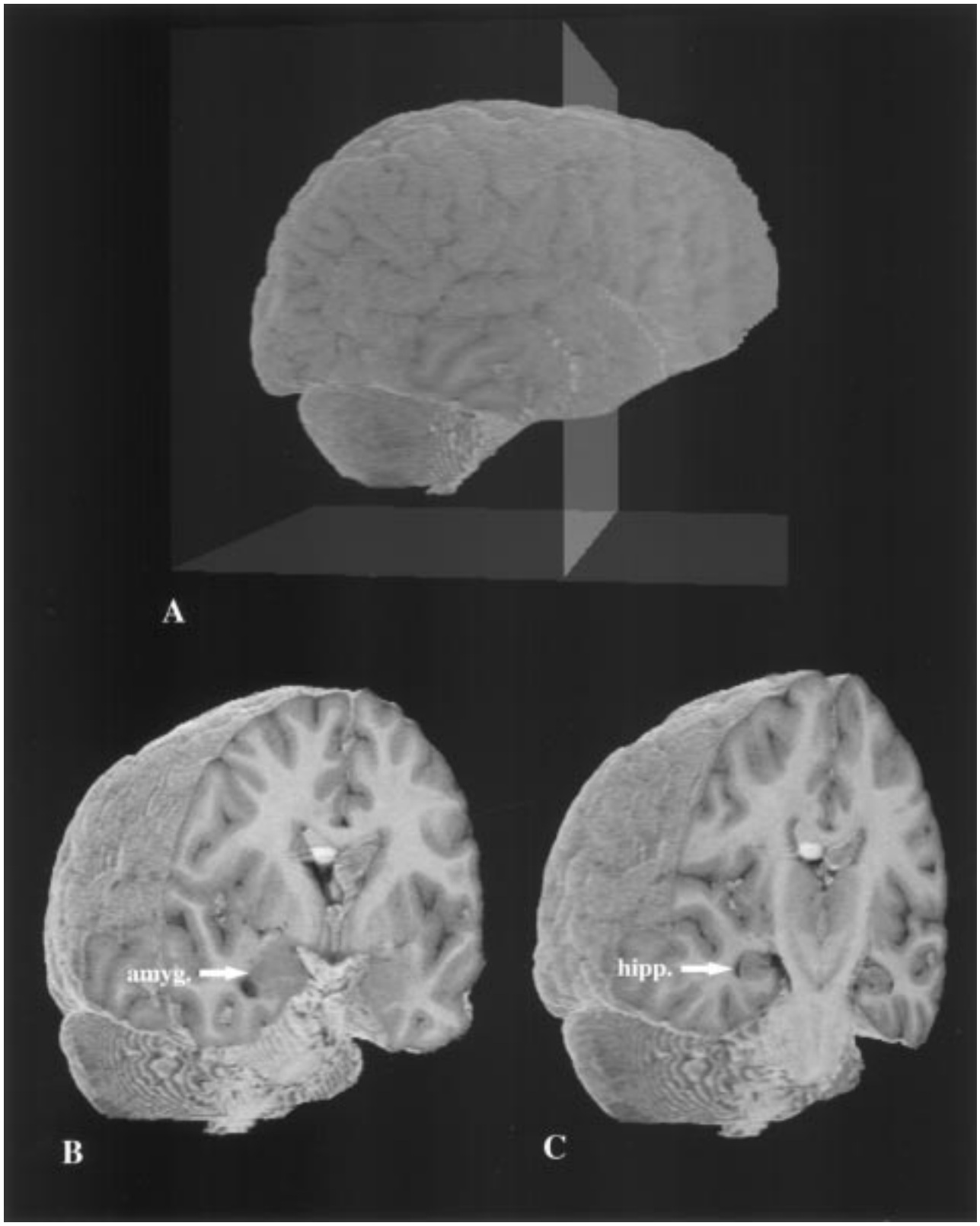

Fig. 4. (Panel A) Three-dimensional reconstructed image using *VirtualSurgery* program from a proton density-weighted MRI scan of the whole brain in Fig. 1. The transverse plane through the 3D image in Panel A represents the location of the virtual cut made through the amygdala displayed in Panel B. A second cut was made further caudal through the hippocampus (Panel C).

on the GE MRI system, it would be necessary to run three separate three-dimensional acquisitions, each with 124 images covering approximately one-third of the brain. The scan time would need to be increased by a factor of three to cover the brain extent, and then by a factor of nine, through increase in NEX, to recover the SNR lost by the decrease in voxel size. This would yield scan time of over 22 hours. Similarly, to acquire the data set with 0.8 mm slice thickness on the GE MRI system, it would be necessary to run two separate three-dimensional acquisitions, each with 124 images covering approximately one-half of the brain. The scan time would need to be increased by a factor of two to cover the brain extent, and then by a factor of four, through increase in NEX, to recover the SNR lost by the decrease in voxel size. This would yield a scan time of 6 hours, 43 minutes, 52 seconds.

Scan times for three-dimensional acquisition can be reduced by orienting the slice selection direction so that the extent of the brain can be covered using as few slices as possible. Typical brain dimensions are just less than 18 cm A/P, 13.0 cm R/L, and 13.5 cm D/V, the latter including the cerebellum. Maximum reduction in scan time is achieved by using sagittal slices, such that the slice selection direction is right to left, the direction of shortest extent of the brain. With this orientation, the FOV would need to be increased slightly to 18 cm to ensure that the anterior/posterior extent was enclosed by the FOV, and 163 slices at 0.8 mm each could cover the A/P extent. A factor of four increase in NEX would be needed to recover the SNR lost by the factor of two reduction in voxel size. This increase in NEX would be reduced somewhat if the MRI system acquires the 163 slices in a single acquisition.

Another suggestion for future studies would be to consider incorporating diffusion tensor sequences. White matter tracks cannot be followed from source to destination in the scans using the current protocol. However, recently developed diffusion-weighted tensor imaging provides visualization of the orientation of white matter tracts, by measuring relative rates of the diffusion of water in three orthogonal directions, and allowing calculation of the six-component diffusion tensor at each voxel. This sequence will be included in future protocols of post-mortem brain analysis. A typical multi-slice diffusion weighted sequence utilizing echo planar imaging requires only 3 minutes, 20 seconds of scan time. It applies 26 combinations of x-, y- and z-diffusion-sensitizing gradient pulses to allow calculation of the diffusion tensor. The proposed protocol will provide images of diffusion anisotropy, maps of the principal and secondary direction, and magnitudes of diffusion directions through the diffusion tensor.

One final consideration would be to increase the field strength of the magnet. High field imaging (e.g., 3.0T) provides a signal-to-noise increase that is roughly linearly proportional to the field strength. Consequently, a 3.0T MRI system provides twice the resolution in the slice select direction (e.g., 0.8 mm instead of 1.6 mm slice thickness) in the same scan time. Higher field causes T1 values to lengthen and become more similar across tissues, and causes T2 values to decrease slightly. Proton density remains the same, but differences in proton density become easier to detect because of the higher SNR. It is expected that at a higher field, the long TR, short TE proton density-weighted sequence will remain optimal. The image contrast produced by this sequence is not affected by the longer and more similar T1s, nor the shorter T2s, yet is fully benefited by the increased magnetization produced by the higher field. A well-known disadvantage of high field *in vivo* imaging is the main field inhomogeneity caused by differences in susceptibility of bone and tissue, and air and tissue. The inhomogeneity causes image distortion and signal loss. Although bone is not present in these specimens, air is present and may introduce a limitation that requires alternate preparation of the specimen to eliminate these interfaces. The three-dimensional fast spin echo sequence minimizes the effect of susceptibility, but reduction in the ETL might be necessary to reduce the effect. At 4.0T and higher, tissue susceptibility becomes proportionally more significant, and penetration of the radio-frequency excitation field becomes another source of signal variation and distortion across the image. Successful and consistent imaging at 4.0T and above will depend on finding methods to minimize the effect of this physical phenomenon.

By incorporating MRI analysis in neuropathological investigations, studies may benefit from a record of the intact brain. A virtual three-dimensional representation of the whole brain may then be resectioned for additional analyses that would not be possible once the brain is blocked and tissue sections are distributed. Providing MRI scans for the autism research community is intended as a resource to maintain a reference database of autistic and control brain tissue.

ACKNOWLEDGMENTS

MRI of the post-mortem human brain at the M.I.N.D. Institute, UC Davis, has now become an in-

tegral part of the Autism Tissue Program. For further information on viewing images, contact ATP director Jane Pickett, Ph.D., at 1-877-333-0999 or ATP@brain bank.org. The authors thank Evan Fletcher, Ph.D. (evan@quark.ucdavis.edu), creator of the Virtual Surgery program; and Neva Corrigan and Sarah Cox for their technical assistance. This work has been supported by a grant from the NIMH 41439 and from the M.I.N.D. Institute.

REFERENCES

Bailey, A., Luthert, P., Dean, A., Harding, B., Janota, I., Montgomery, M., Rutter, M., & Lantos, P. (1998). A clinicopathological study of autism. *Brain, 121*(Pt 5), 889–905.

Blamire, A. M., Rowe, J. G., Styles, P., & McDonald, B. (1999). Optimising imaging parameters for post-mortem MR imaging of the human brain. *Acta Radiology, 40*(6), 593–597.

Bobinski, M., de Leon, M. J., Wegiel, J., Desanti, S., Convit, A., Saint Louis, L. A., Rusinek, H., & Wisniewski, H. M. (2000). The histological validation of post-mortem magnetic resonance imaging-determined hippocampal volume in Alzheimer's disease. *Neuroscience, 95*(3), 721–725.

Jack, C. R., Jr., Petersen, R. C., O'Brien, P. C., & Tangalos, E. G. (1992). MR-based hippocampal volumetry in the diagnosis of Alzheimer's disease. *Neurology, 42*(1), 183–188.

Nagara, H., Inoue, T., Koga, T., Kitaguchi, T., Tateishi, J., & Goto, I. (1987). Formalin fixed brains are useful for magnetic resonance imaging (MRI) study. *Journal of Neurological Science, 81*(1), 67–77.

Nixon, J. R., Miller, G. M., Okazaki, H., & Gomez, M. R. (1989). Cerebral tuberous sclerosis: Postmortem magnetic resonance imaging and pathologic anatomy. *Mayo Clinical Proceedings, 64*(3), 305–311.

Piven, J., Arndt, S., Bailey, J., & Andreasen, N. (1996). Regional brain enlargement in autism: A magnetic resonance imaging study. *Journal of the American Academy of Child and Adolescent Psychiatry, 35*(4), 530–536.

Saitoh, O., & Courchesne, E. (1998). Magnetic resonance imaging study of the brain in autism. *Psychiatry and Clinical Neuroscience, 52*(Suppl), S219–222.

Scarpelli, M., Salvolini, U., Diamanti, L., Montironi, R., Chiaromoni, L., & Maricotti, M. (1994). MRI and pathological examination of post-mortem brains: The problem of white matter high signal areas. *Neuroradiology, 36*(5), 393–398.

Seab, J. P., Jagust, W. J., Wong, S. T., Roos, M. S., Reed, B. R., & Budinger, T. F. (1988). Quantitative NMR measurements of hippocampal atrophy in Alzheimer's disease. *Magnetic Resonance Medicine, 8*(2), 200–208.

Tovi, M., & Ericsson, A. (1992). Measurements of T1 and T2 over time in formalin-fixed human whole-brain specimens. *Acta Radiology, 33*(5), 400–404.